ACS APPLIED MATERIALS & INTERFACES

Research Article

www.acsami.org

Conjugated Polyelectrolyte-Sensitized TiO_2 Solar Cells: Effects of Chain Length and Aggregation on Efficiency

Zhenxing Pan, Gyu Leem, Seda Cekli, and Kirk S. Schanze*

Department of Chemistry and Center for Macromolecular Science and Engineering, University of Florida, P.O. Box 117200, Gainesville, Florida 32611-7200, United States

Supporting Information

ABSTRACT: Two sets of conjugated polyelectrolytes with different molecular weights (M_n) in each set were synthesized. All polymers feature the same conjugated backbone with alternating (1,4-phenylene) and (2,5-thienylene ethynylene) repeating units, but different linkages between the backbone and side chains, namely, oxy-methylene (-O-CH_2-) (P1-O-*n*, where *n* = 7, 9, and 14) and methylene (-CH_2-) (P2-C-*n*, *n* = 7, 12, and 18). They all bear carboxylic acid moieties as side chains, which bind strongly to titanium dioxide (TiO_2) nanoparticles. The two sets of polymers were used as light-harvesting materials in dye-sensitized solar cells. Despite the difference in molecular weight, polymers within each set have very similar light absorption properties. Interestingly, under the same working conditions, the overall cell efficiency of the P1-O-*n* series increases with a decreasing molecular weight while the efficiency of the P2-C-*n* series remains constant regardless of the molecular weight. Steady state photophysical measurements and dynamic light scattering investigation prove that P1-O-*n* polymers aggregate in solution while P2-C-*n* series are in the monomeric state. In P1-O-*n* series, a higher-molecular weight polymer results in a larger aggregate, which reduces the amount of polymers that are adsorbed onto TiO_2 films and overall cell efficiency.

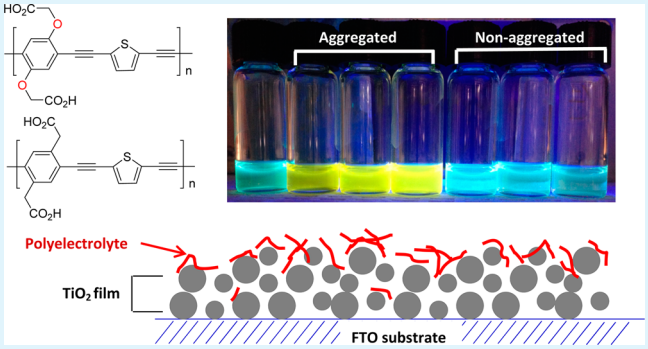

KEYWORDS: *conjugated polyelectrolytes, aggregation, cell efficiency, dye-sensitized solar cells*

INTRODUCTION

Dye-sensitized solar cells (DSSCs) are one of the most important low-cost alternatives to conventional silicon-based inorganic solar cells.[1,2] Since the first report of the technology, it has drawn significant attention from the scientific community.[3] A great deal of effort has been spent on understanding the fundamental problems, improve the overall cell efficiency, and explore the possibility of commercialization.[4,5] There are several advantages of the DSSC format over traditional solar cells, which include the use of low-cost materials, mechanical flexibility, and the possibility of large scale manufacture. Initially, metal−organics, in particular ruthenium and metalloporphyrin complexes, have been utilized as sensitizers and demonstrated power conversion efficiency (PCE) as high as 13% and incident photon to current efficiency (IPCE) of >85%.[6] Meanwhile, donor−π-bridge−acceptor (D−π−A) type organic dyes are emerging as a new class of sensitizers, and upon careful structural design, they can also attain efficiencies matching that of inorganic dyes.[7,8] Very recently, highly efficient hybrid perovskite cells have been made, achieving efficiency as high as 19.3%.[9]

In the past two decades, conjugated polyelectrolytes (CPEs) have drawn significant attention. CPEs are π-conjugated polymers with ionic or ionizable functional groups on a π-conjugated backbone. Some of the key advantages of CPEs are strong light absorption in the visible region, a tunable bandgap, and processability from green solvents.[10,11] Despite their advantages, the application of CPEs as sensitizers in DSSCs has rarely been studied. Our research group has reported several studies focused on the use of CPEs as sensitizers in DSSCs.[12−15] In previously reported work on CPE-sensitized DSSCs, some effort has focused on the design of novel donor−acceptor (D−A) structured CPEs, which are believed to facilitate intramolecular charge transfer from the donor to acceptor resulting in a smaller optical bandgap.[16−18] Such polymers show broad absorption and large extinction coefficients, that are crucial to efficient light harvesting. However, recently, several research groups have reported that polymer chain length can also have a significant impact on the overall cell performance when CPEs are used as the sensitizers for DSSCs.[18,19] This effect was attributed to the decrease in the cell efficiency of high-molecular weight polymers because of their large size, which lowers their ability to diffuse into the mesoporous TiO_2 films and to cover the surface effectively. Similarly, previous studies show that the overall efficiency of

Received: May 13, 2015
Accepted: July 7, 2015
Published: July 7, 2015

DOI: 10.1021/acsami.5b04162
ACS Appl. Mater. Interfaces 2015, 7, 16601−16608

Chart 1. Structures of P1-O-*n*, P2-C-*n*, and the Model Oligomer

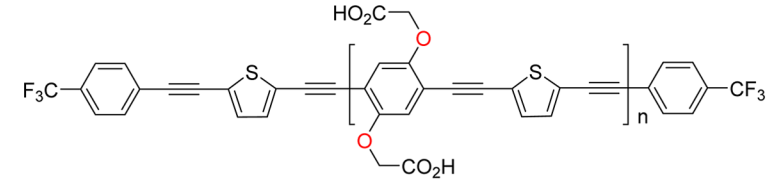

P1-O-n, n = 7, 9, 14

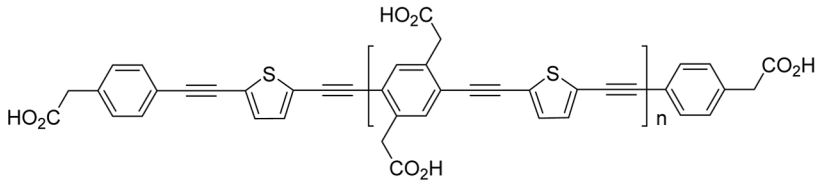

P2-C-n, n = 7, 12, 18

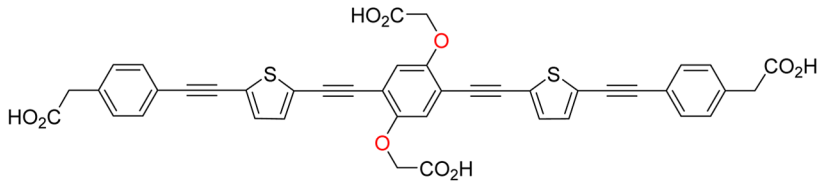

Model

dendrimer-sensitized cells also decreases with an increasing dendrimer size.[20,21]

In this work, we study the relationship between the overall cell efficiency and molecular weight of two series of CPEs that feature the same conjugated backbone with alternating 1,4-phenylene and 2,5-thienylene ethynylene repeating units (Chart 1). In this study, the two series of CPEs differ in a subtle yet important structural feature. In particular, the linkage between the polymer backbone and the carboxylic acid side chains is different: alkoxy (e.g., -O-CH_2-) for the P1-O-*n* series and alkyl (e.g., -CH_2-) for the P2-C-*n* series [*n* is the degree of polymerization (DP)]. This difference is significant, because in previous work we have shown that the molecular structure of the linker has an influence on the propensity of the polymers to aggregate in solution.[22,23] The (phenylene ethynylene)-*alt*-(thienylene ethynylene) polymer backbone structure was chosen in part because of the ease of synthesizing the monomers and the ability to control the molecular weight in the Sonogashira step growth polymerization via an end capping strategy.[24] The carboxylic acid pendant groups facilitate adsorption of the polymers onto mesoporous TiO_2 films and ensure that polymeric chromophores are in the proximity of the surface of TiO_2, enhancing charge injection. Steady state absorption and emission spectra of the polymers were obtained to compare their photophysical properties in solution, and dynamic light scattering was applied to characterize their aggregation. When they are applied in DSSCs, the efficiency of P1-O-*n*-sensitized cells depends strongly on the polymer molecular weight, while the efficiency of the P2-C-*n*-sensitized cells does not vary with molecular weight. Our results herein clearly demonstrate that a minor change in side chain could have a significant impact on the aggregation behaviors of polymers and ultimately on their performance as sensitizers in TiO_2-based DSSCs.

EXPERIMENTAL PROCEDURES

Materials and Synthesis. All materials were purchased from commercial suppliers and used as received unless otherwise specified. Detailed synthetic procedures and characterization of compounds and polymers are provided in the Supporting Information.

Instrumentation and Methods. ^{1}H and ^{13}C NMR spectra were recorded on a Varian Mercury 300, Gemini 300, or Inova 500 MHz spectrometer. Chemical shifts were referenced to the residual solvent peaks. High-resolution mass spectrometry was performed on a Bruker APEX II 4.7 T Fourier transform ion cyclotron resonance mass spectrometer (Bruker Daltonics). Gel permeation chromatography (GPC) data were collected on a system composed of a Shimadzu LC-6D pump, an Agilent mixed-D column, and a Shimadzu SPD-20A photodiode array (PDA) detector, with tetrahydrofuran (THF) as the eluent at a flow rate of 1 mL/min. The system was calibrated against linear narrow dispersed polystyrene standards in THF.

UV−visible absorption measurements were taken on a Shimadzu UV-1800 dual-beam absorption spectrophotometer. Photoluminescence spectra were recorded on a spectrofluorimeter from Photon Technology International (PTI). Photoluminescence lifetimes were obtained by time-correlated single-photon counting (TCSPC) using a Fluo Time 100 instrument (Picoquant), and excitation was provided using a PDL 800-B picosecond pulsed diode laser (375 nm). Film transient absorption measurements were conducted on a home-built apparatus. The excitation wavelength was generated by a Continuum Surelite OPO Plus pumped with the third harmonic (355 nm) of a Continuum Surelite II-10 Nd:YAG laser. A xenon arc lamp was used as a probe source. A Triax 180 monochromator and Si-amplified photodetector from Thorlabs (PDA8A) were used for detection at a single wavelength. Films were submerged in sealed cuvettes containing 0.1 M $LiClO_4$ in acetonitrile and degassed with Ar for 30 min before measurements were taken.

Dynamic light scattering (DLS) characterization was performed on a Zetasizer Nano (Malvern Instruments, Worcestershire, U.K.) at 25 °C. The concentration of the samples was adjusted to 0.1 mg/mL. Three measurement cycles were run for each sample. The data were averaged from 10 light scattering periods of 10 s for each cycle. Average diameter values were calculated using the Malvern Instruments DTS software.

DOI: 10.1021/acsami.5b04162
ACS Appl. Mater. Interfaces 2015, 7, 16601−16608

Dye-Sensitized Solar Cell Fabrication and Testing. The nanocrystalline titanium dioxide (TiO_2) electrode (on fluorine-doped SnO_2 substrates) and the platinized counter electrode were prepared according to a literature method.[25] Two holes were drilled into the counter electrode to allow electrolyte to be injected into the sealed cell compartment. A solution of 0.1 mg/mL P1-O-*n* or P2-C-*n* polymer in dimethylformamide (DMF) was stirred for 24 h, and then the FTO/TiO_2 electrodes were immersed in the solution. After the electrodes had been soaked for 36 h, the electrodes were rinsed with dry DMF and acetone to remove unabsorbed polymer, and then the films were placed into a vacuum chamber for 2 h to remove all residual solvents. The counter electrode and the FTO/TiO_2 anode were sealed together with a 25 μm Surlyn spacer (Solaronix Meltonix 1170-25). The electrolyte solution containing 0.05 M I_2, 0.1 M LiI, 0.6 M 1-methyl-3-(*n*-propyl)imidazolium iodide, and 0.5 M 4-*tert*-butylpyridine in butyronitrile was injected into the sealed device by using the holes in the counter electrode.

For characterization of the IPCE response of the solar cells, an Oriel Cornerstone monochromator was used as a light source, and the device current response was recorded under short-circuit conditions at 10 nm intervals using a Keithley 2400 source meter. The light intensity at each wavelength was calibrated with an energy meter (S350, UDT Instruments). The current−voltage characteristics of the cells were measured with a Keithley 2400 source meter under illumination with AM1.5 simulated solar light (100 mW/cm^2).

RESULTS AND DISCUSSION

Structures, Synthesis, and Characterization. In this study, two series of polymers, P1-O-*n* and P2-C-*n*, that feature the same conjugated backbone with alternating (1,4-phenylene) and (2,5-thienylene ethynylene) repeating units, but different linkages between the backbone and side chains, namely, alkyoxy (-O-CH_2-) and alkyl (-CH_2-), respectively, were synthesized. For comparison, an oligomer that has a structure similar to the polymers was prepared as a model compound. The structures of the polymers and oligomer are shown in Chart 1. All the samples feature carboxylic side groups that help improve polymer solubility in solution and serve as anchoring groups for adsorption on TiO_2.

The polymers were synthesized via the "precursor route" in which the carboxy groups were protected as dodecyl esters.[24,26] The ester-protected polymers were hydrolyzed and then acidified to afford the carboxylic acid-substituted polymers (see Scheme S1 of the Supporting Information). The polymer chain length was controlled by applying the "end capping" strategy during the Sonogashira Pd-catalyzed step growth polymerization to the ester-protected polymers. In this process, monofunctional end-capping groups were added to the reaction mixture, changing the stoichiometric ratio of the monomers.[24,27] The molecular weight (M_n) and polydispersity (PDI) of the resulting dodecyl ester-protected polymers were determined, and the number of repeat units of the polymers was estimated from the M_n values. The results obtained by GPC and NMR methods are in good agreement and are listed in Table 1. The polydispersity index (PDI) for P1-O-*n* is in the range of 1.53−1.74, while that of P2-C-*n* is roughly ∼2, which is typical for step growth polymerization.[27]

Dynamic Light Scattering: Aggregation of P2-O Series. Dynamic light scattering has been widely used to characterize the size of polyelectrolyte chains and aggregates in solution.[28,29] In this work, polymer solutions were prepared in DMF and the concentration was set to 0.1 mg/mL. The DLS histograms are shown in the Supporting Information, and the results are summarized in Figure 1. First, the model compound is smaller (∼2 nm) than the polymer samples. Next, it is found

Table 1. Molecular Weights of P1-O-*n*, P2-C-*n*, and the Model Compound

	M_n (g/mol)[a]	M_w (g/mol)[a]	PDI	DP (GPC)	DP (NMR)
Model	866	866	–	–	–
P1-O-14-ester	9900	17200	1.74	14	13
P1-O-9-ester	6600	10200	1.53	9	8
P1-O-7-ester	5000	7700	1.55	7	6
P2-C-18-ester	13000	26000	1.98	18	17
P2-C-12-ester	8400	17000	2.00	12	11
P2-C-7-ester	5100	9500	1.87	7	7

[a]Polystyrene standards used.

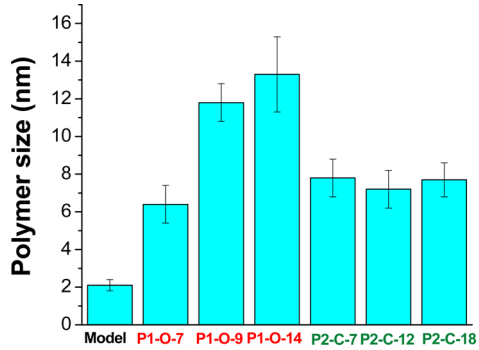

Figure 1. Dynamic light scattering of samples in DMF at a concentration of 0.1 mg/mL.

that the size of the P2-C series is relatively constant (∼7 nm), regardless of M_n. It is well-known that the radius of gyration of polyelectrolytes remains constant for chains having a wide range of molecular weights, which explains the trend for the P2-C series.[30,31] By contrast, the effective scattering size of the P1-O series increases substantially with molecular weight, ranging from ∼6 nm for P1-O-7 to ∼13 nm for P1-O-14. The increasing particle size for P1-O series is very likely to be caused by aggregation of individual chains into particles that consist of multiple chains that are held together by supramolecular interactions (e.g., π-stacking, H-bonding, etc.). The higher-molecular weight polymers tend to form larger aggregates, thereby increasing the particle size.[24]

Previous work from our lab reveals that the molecular structure of the side chain linkages can strongly influence the tendency of PPE type conjugated polyelectrolytes to aggregate in solution.[22,23,32] In particular, polymers with -O-CH_2- linkages have a stronger tendency to aggregate in solution, whereas polymers having -CH_2- linkages show a surprisingly weaker tendency to aggregate. The difference is likely due to the electronic effect of the oxygen atoms leading to enhanced dispersion interactions between chains and/or differences in steric and torsional interactions arising from the difference in chain size and sterics for the -CH_2- and -O-CH_2- linker.[23]

Furthermore, molecular dynamics study of the P2-C-*n* chains shows that they adopt a helical conformation rather than wormlike conformations in solution.[33] An atomic force microscopy (AFM) study of P2-C-*n* chains adsorbed on single-crystal (anatase) TiO_2 showed that the effective diameter of single (helical conformation) polymer chains is 47 ± 3 Å.[32] Interestingly, the size of the P2-C series in solution as monitored by DLS is consistent with the previously reported AFM-determined size for the same polymers adsorbed on TiO_2 (7 nm vs 5 nm). These findings support the premise that P2-C-

DOI: 10.1021/acsami.5b04162
ACS Appl. Mater. Interfaces 2015, 7, 16601−16608

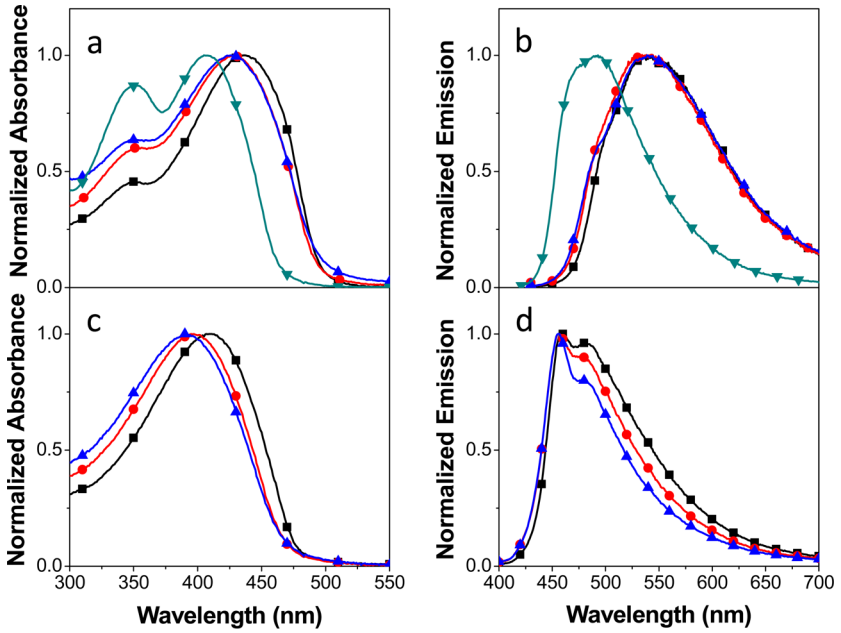

Figure 2. Ground state absorption and fluorescence spectra. (a) Normalized UV−visible absorption and (b) emission spectra of P1-O-14 (black squares), P1-O-9 (red circles), P1-O-7 (blue triangles), and the model compound (green triangles). (c) Normalized UV−visible absorption and (d) emission spectra of P2-C-18 (black squares), P2-C-12 (red circles), and P2-C-7 (blue triangles). All measurements were taken in DMF at a concentration of 0.1 mg/mL.

Table 2. Summary of Polymer Molecular Weights and Photophysical Data

	M_n	PDI	DP	λ_{abs} (nm)	ε ($\times 10^4$ cm^{-1} M^{-1})	λ_{em} (nm)	φ_{fl}[a]
P1-O-14	9900	1.7	14	432	3.8	542	0.071
P1-O-9	6600	1.5	9	425	3.5	531	0.091
P1-O-7	5000	1.6	7	424	2.9	528	0.14
Model	866	–	–	408	9.9	470	0.39
P2-C-18	13000	2.0	18	407	5.9	457	0.13
P2-C-12	8400	2.0	12	398	5.5	456	0.12
PC-C-7	5100	1.9	7	388	5.1	456	0.12

[a]Measurements in pH 8 water with quinine sulfate in 0.1 M H_2SO_4 as a standard, where φ_{fl} = 0.545.

n polymers are more likely to be monomeric in solution while the P1-O-*n* polymers are aggregated.[23,24,34]

Optical Properties in Solution. Steady state UV−visible absorption and emission spectra of the polymers and the model compound were measured in DMF (c = 50 μM based on polymer repeat units), and the spectra are illustrated in Figure 2. Molar extinction coefficients and fluorescence quantum yields are listed in Table 2. As shown in panels a and c of Figure 2, the absorption spectra are similar for both series with absorption maxima (λ_{abs}) red-shifting as the molecular weight increases, likely because of the increase in the effective conjugation length (424, 425, and 432 nm for P1-O-7, P1-O-9, and P1-O-14, respectively; 388, 398, and 407 nm for P2-C-7, P2-C-12, and P2-C-18, respectively). Note that the absorption of the P1-O-*n* set is red-shifted approximately 25 nm compared to that of the P2-C-*n* series. This is due to the effect of the -O-R substituents on the phenylene rings, which because of their electron donating character increase the energy of the HOMO, leading to a decrease in the HOMO−LUMO (optical) gap.[23] The absorption maximum of the model compound is blue-shifted ∼20 nm compared to that of the P1-O series, because its conjugation length is shorter than those of any of the polymers.

Fluorescence spectra of P1-O-*n* and P2-C-*n* are shown in panels b and d of Figure 2, respectively. The fluorescence of the P1-O-*n* series appears as a broad, unstructured band, and the band maximum is relatively constant across the series, despite the substantial increase in DP. The emission from P1-O-*n* also exhibits an approximately 100 nm Stokes shift. By contrast, the fluorescence of the P2-C-*n* polymers appears as a narrower band, with a vibronic shoulder, the intensity of which decreases with increasing DP. The spectra of the P2-C-*n* series are consistent with the polymer chains being molecularly dissolved; however, the significant Stokes shift and broad nature of the spectra of the P1-O-*n* set strongly suggest that these polymers are aggregated in the DMF solution.[35,36] The broad and red-shifted fluorescence spectra are consistent with emission from an interchain (aggregate) state.[35] The fluorescence quantum yields (φ_{fl}) also reflect the difference in the solution state of the two sets of polymers. In particular, φ_{fl} values for the P2-C-*n* polymers are moderate and relatively constant across the series, whereas φ_f decreases with an increasing DP for the P1-O-*n* series.

Taken together, the DLS and optical spectroscopy data for the two families of polymers strongly suggest that in DMF solution, the -O-CH_2-substituted family is aggregated in solution, with the degree of aggregation increasing with DP. On the other hand, the -CH_2-linked series is likely to be molecularly dissolved in DMF under the same conditions. The

DOI: 10.1021/acsami.5b04162
ACS Appl. Mater. Interfaces 2015, 7, 16601−16608

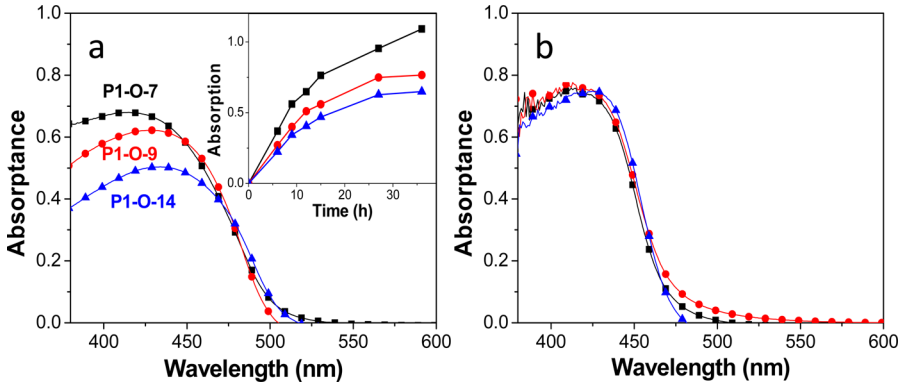

Figure 3. Absorptance ($1 - 10^{-A}$) of TiO_2/polymer films following deposition from DMF solutions. (a) Absorptance of P1-O-*n* films and time-dependent absorption (inset): P1-O-7 (black squares), P1-O-9 (red circles), and P1-O-14 (blue triangles). (b) Absorptance of P2-C-*n* films: P2-C-7 (black squares), P2-C-12 (red circles), and P2-C-18 (blue triangles).

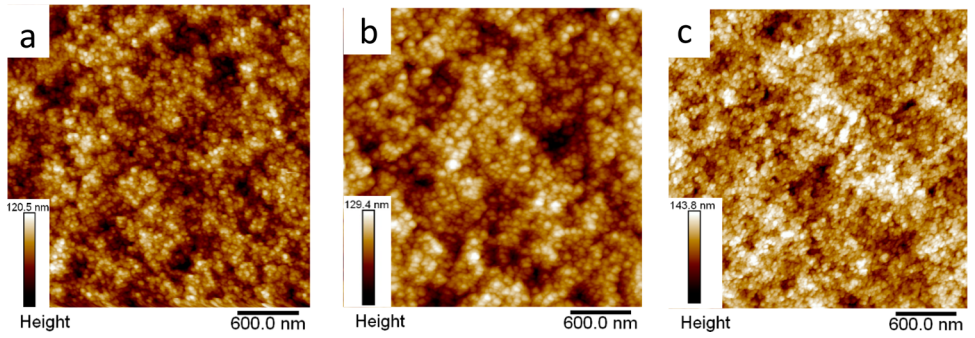

Figure 4. AFM images of mesoporous TiO_2 films: (a) pristine film, (b) P2-C-18-coated film, and (c) P1-O-14-coated film. Root mean square (rms) values for uncoated TiO_2, P2-C-18, and P1-O-14 films are 17.4, 18.6, and 20.5 nm, respectively.

reason for the difference in solution properties of the two families of polymers is uncertain, but as suggested in earlier work,[23] it may be related to electronic or structural differences arising from the nature of the side chain linkers on the phenylene units.

TiO_2 Film Characterization, Polymer Adsorption, and Charge Injection. For the films used in this investigation, the TiO_2 particles have an average size of ~17 nm and the film thickness is ~13 μm, as assessed by scanning electron microscopy [SEM (see Figure S1 of the Supporting Information)]. UV−visible absorption spectroscopy was used to monitor adsorption of the P1-O-*n* and P2-C-*n* polymers onto the TiO_2 films from a DMF solution. The uncoated TiO_2 films have little absorption beyond 380 nm, and all the films have very similar thicknesses according to SEM images. For polymer adsorption, 0.1 mg/mL polymer was added to DMF, and the mixture was stirred for 24 h. Then the TiO_2-coated substrates were soaked in the polymer/DMF solutions for 36 h. The UV−visible absorption of the resulting polymer coated films was measured, and the absorptance of films (absorptance = $1 - 10^{-A}$, where A is absorption) is plotted in Figure 3. Quite interestingly, it is evident from these data that the absorptance of the P1-O-*n*/TiO_2 films decreases with DP, suggesting that the surface coverage decreases as DP increases. In contrast, the P2-C-*n*/TiO_2 films exhibit almost identical peak absorptance, and the peak absorptance observed is greater, suggesting higher overall surface coverage.

To further characterize the film absorption properties of P1-O-*n* series, time-dependent adsorption measurements were performed. A set of TiO_2 films with the same thickness were soaked in P1-O-*n* solutions in DMF with the same concentration for various periods of time, and the film absorption was measured. The absorption values at 440 nm were recorded, and the calculated absorptance is plotted in Figure 3a (inset). Note that the polymer coverage for all of the films increases with time. The most significant enhancement is seen during the first 15 h, and it reaches a plateau after 30 h, indicating saturation of TiO_2 surface coverage. Note that, at any given time, the film absorption increases with decreasing DP.

The surface coverage of the polymer on the TiO_2 films (moles per square centimeter) was quantified by calculating the molar surface concentration, Γ, which is calculated according to the equation $\Gamma = A/\varepsilon$, where A is the film absorption and ε is the molar extinction coefficient (on a polymer repeat unit basis). The key assumption in this calculation is that the polymers' molar extinction coefficients are the same for the solution and on the TiO_2 surface. The calculated surface coverage for the polymer/TiO_2 films is on the order of 10^{-8} mol/cm^2 [polymer repeat units (see Figure S2 of the Supporting Information)]. For the P1-O-*n* series, the surface coverage decreases with an increasing DP, ranging from 3.5 to 1.5×10^{-8} mol/cm^2, whereas for the P2-C-*n* series, the surface coverage is ~2.5×10^{-8} mol/cm^{-2} and is independent of DP. The surface coverage is lower compared to those of many small metal−organic or organic dyes, ~10^{-7} mol/cm^{-2}.[20,21,37]

The surface topography of the mesoporous TiO_2 films with and without the adsorbed polymers was characterized by AFM. Typical images for the uncoated and polymer coated films are shown in Figure 4. For the uncoated and P2-C-18-coated films (panels a and b of Figure 4, respectively), the TiO_2

DOI: 10.1021/acsami.5b04162
ACS Appl. Mater. Interfaces 2015, 7, 16601−16608

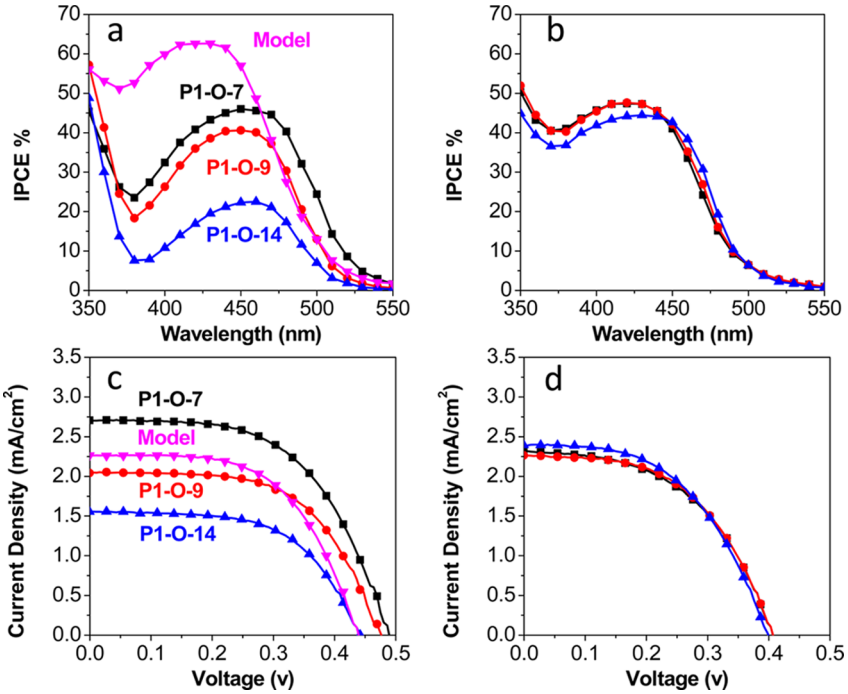

Figure 5. IPCE and current−voltage (J−V) character of polymer cells. (a) IPCE and (b) J−V curves of P1-O-*n* and the model compound: P1-O-7 (black squares), P1-O-9 (red circles), P1-O-14 (blue triangles), and the model compound (magenta triangles). (c) IPCE and (d) J−V curves of P2-C-*n*: P2-C-7 (black squares), P2-C-12 (red circles), and P2-C-18 (blue triangles).

nanoparticles in the film are clearly resolved, and it is evident that the P2-C-18 coating has little effect on film morphology. This suggests that P2-C-18 provides a conformal coating and is smoothly adsorbed within the mesoporous film. Interestingly, the P1-O-14-coated film has a "rougher" appearance (Figure 4c), and the overall height difference in the AFM images is substantially greater. This is consistent with the P1-O-14 providing a more complex, aggregated coating, as would be expected if the polymer is aggregated in solution and the aggregates deposit onto the surface during adsorption. The difference in surface topography for the three films was characterized by determining the root-mean-square (rms) roughness of the surface from the AFM images. Compared to the rms value of bare TiO_2 (17.4 nm), that of the P2-C-18-sensitized film increased slightly (from 17.4 to 18.6 nm), indicating that P2-C-18 successfully adsorbs onto the TiO_2 particles and there is no obvious aggregation on the film surface. However, the rms value of the film sensitized with P1-O-14 (20.5 nm) is significantly higher than that of bare TiO_2, and this further substantiates the premise that polymer aggregates are adsorbed on the surface of the mesoporous film. Considering the fact that the P2-O-*n* series show lower absorptance, which means less polymer is adsorbed onto the film, we hypothesize that the aggregated P1-O-*n* will block the mesopores on the film surface, preventing the polymer from diffusing deep into the mesoporous film. Taken together, the results from UV−visible absorption and AFM clearly establish the fact that the aggregation status of the polymer in solution determines the film morphology and affects the total amount of polymer that can be absorbed into the mesoporous films.

Transient absorption spectroscopy (TA) experiments were performed on P1-O-*n*-sensitized films to gain insight into charge injection and recombination kinetics in the polymer-sensitized films. These experiments were conducted using 355 nm pulses from a Nd:YAG laser (10 ns pulse width) for excitation. The polymer-sensitized films were contained in sealed cuvettes containing 0.1 M $LiClO_4$ in acetonitrile and degassed with argon for 30 min prior to measurements. Following laser excitation, strong transient absorption throughout the visible and near-infrared regions is observed, with a band maximum at ∼675 nm (Figure S3 of the Supporting Information). The absorption is attributed to the oxidized state of the polymers produced by injection of charge into the TiO_2 conduction band. Interestingly, the intensity of the transient absorption signal for the P1-O-*n* series decreases with an increasing DP, which is consistent with the trend of decreasing polymer surface coverage with increasing DP. Charge recombination occurs between the polymer cations and the TiO_2 conducting band electrons, and the signal decay kinetics were measured at 650 nm and are plotted in Figure S3 of the Supporting Information. Charge recombination occurs on a time scale of 150−200 μs, which is somewhat less than observed for metal complex sensitizers under similar conditions.[38−40]

Polymer-Sensitized TiO_2 Solar Cells. The scope of this work is to understand the effects of polymer molecular weight and aggregation on cell performance, as opposed to achieving high cell efficiency. Consequently, all cells were fabricated and characterized under the same conditions without seeking to optimize overall performance (e.g., varying electrolyte, additives, etc.). The active area of the cells is ∼0.2 cm^2. Three different batches of devices were prepared for each sample, and the results were consistent in every case.

Plots of the incident photon to current efficiency (IPCE) of both P1-O-*n* and P2-C-*n* series of polymers are plotted in Figure 5. Interestingly, a significant decrease in the peak IPCE is observed for the P1-O-*n* series with increasing DP, whereas the IPCE for the P2-C-*n* varies little despite the difference in DP (Figure 5a). In the P1-O-*n* series, P1-O-7, which has the lowest DP, exhibits the highest peak IPCE value (∼50%) and

DOI: 10.1021/acsami.5b04162
ACS Appl. Mater. Interfaces 2015, 7, 16601−16608

the IPCE value decreases with an increasing DP. The IPCE of P1-O-14 is only approximately half of that of P1-O-7 (~25%), consistent with the lower overall light harvesting efficiency for this polymer. In contrast, all of the P2-C-*n* polymers exhibit a comparably efficient peak IPCE value of ~48%, indicating that the light harvesting efficiency and charge injection are quite efficient under short-circuit conditions. The trend in peak IPCE value is consistent with the film absorptance (Figure 3). The difference in current density of devices is also due to the change in the total amount of polymers adsorbed. Although the model oligomer shows the highest peak IPCE value (~65%), the IPCE spectral response is narrower, consistent with the blue-shifted absorption of the model.

The same correlation between DP and efficiency can be observed in the *J*−*V* characteristics of the P1-O series (Figure 5b,d), where P1-O-7 shows the highest open-circuit voltage value (V_{oc} = 0.49 V) and short-circuit current (J_{sc} = 2.70 mA/cm^2) and P1-O-14 has the lowest V_{oc} (0.45 V) and J_{sc} (1.56 mA/cm^2). This is likely to be caused by polymer aggregation, which affects surface coverage: less aggregated samples can better cover the TiO_2 surface. A better covered film reduces the rate of charge recombination between electrons in the conducting band of TiO_2 and the I^-/I_3^- redox couple or polymer cations at the interface of the TiO_2 particle, thus increasing the open-circuit voltage and short-circuit current.[39,41] The P2-C-*n* polymers all have the same V_{oc} and J_{sc} but have V_{oc} and J_{sc} values somewhat lower than those of P1-O-7; this latter effect likely arises because of the blue-shifted absorption of the P2-C-*n* series, which limits their ability to harvest visible light.[6] Although the model compound does not aggregate, the surface coverage is less efficient than that of P1-O-*n* polymers and a lightly lower V_{oc} is observed.

Table 3 summarizes the solar cell characteristics of the entire family of polymers studied. In addition, Table 3 contains

Table 3. Summary of Cell Performance[a]

	V_{oc} (V)	J_{sc} (mA/cm^2)	FF (%)	IPCE$_{max}$ (%)	APCE$_{max}$ (%)[b]	η_{cell} (%)
P1-O-7	0.49	2.70	55.8	46.0	99.2	0.74
P1-O-9	0.48	2.05	58.3	40.6	88.8	0.57
P1-O-14	0.45	1.56	57.7	24.4	45.2	0.40
Model	0.44	2.26	57.4	62.6	---	0.57
PC-C-7	0.41	2.32	49.9	47.4	73.0	0.47
P2-C-12	0.41	2.26	52.1	47.6	71.8	0.48
P2-C-18	0.40	2.39	50.1	47.4	65.2	0.49

[a]Three cells for each polymer were made, and the all the values are average values. [b]Calculated using the equation APCE = IPCE$_{max}$/absorptance.

calculated values of absorbed light to photon current efficiency (APCE or internal quantum efficiency), and some interesting trends are seen in these data. In particular, the APCE varies strongly across the P1-O-*n* series, with the shortest chain polymer exhibiting a nearly quantitative internal quantum efficiency. However, for this series as the DP increases, the APCE falls significantly to a value below 50%. By contrast, for the P2-C-*n* series, the APCE is relatively constant at ~70%. The strong variation across the P1-O-*n* series strongly suggests that the aggregation in the longer chain polymers leads to a significant reduction in the efficiency of charge injection. This correlates with earlier work we reported in collaboration with Sambur and Parkinson, where it was found that the APCE was negatively affected under conditions where aggregated polymers could be observed at a single-crystal TiO_2 interface by AFM.[33]

CONCLUSION

Two series of carboxylic acid-functionalized conjugated polymers featuring the same alternating (1,4-phenylene) and (2,5-thienylene ethynylene) repeat units, but different DPs, were synthesized and utilized as sensitizers in mesoporous TiO_2 dye-sensitized solar cells. Dynamic light scattering and steady state photophysical results reveal that the P1-O-*n* series that feature alkoxy (-O-CH_2) linkers between the backbone and the carboxylic acid groups are aggregated in solution, with the size of the aggregates increasing with DP. By contrast, the P2-C-*n* series that feature methylene (-CH_2-) linkers appear to be molecularly dissolved in solution. Interestingly, study of the adsorption of the polymers onto mesoporous TiO_2 films reveals that the aggregation state of the polylmers in solution has a strong influence on the film morphology of the polymer-adsorbed films, and it also affects the effective surface coverage by the polymer, as well as the light harvesting efficiency of the polymer-sensitized mesoporous TiO_2 films. As a result, the IPCE and overall solar conversion efficiency of DSSCs that are based on the P1-O-*n* series decrease with an increasing DP, whereas the DSSC performance of DSSCs P2-C-*n* polymers is independent of DP. The reason for the difference in the propensity of the two series of polymers to aggregate is an open question; however, the results reported here clearly establish the negative consequences that polymer aggregation can have on their performance in DSSCs based on mesoporous metal oxide films.

ASSOCIATED CONTENT

Supporting Information

Detailed description of polymer synthesis, TiO_2 film characterization, dynamic light scattering data, and transient absorption spectra and kinetics of polymer-sensitized TiO_2 films. The Supporting Information is available free of charge on the ACS Publications website at DOI: 10.1021/acsami.5b04162.

AUTHOR INFORMATION

Corresponding Author

*E-mail: kschanze@chem.ufl.edu.

Notes

The authors declare no competing financial interest.

ACKNOWLEDGMENTS

This work was partially supported by the National Science Foundation (Grant CHE-1151624).

REFERENCES

(1) Grätzel, M. Dye-Sensitized Solar Cells. *J. Photochem. Photobiol., C* **2003**, *4*, 145−153.
(2) Hagfeldt, A.; Boschloo, G.; Sun, L.; Kloo, L.; Pettersson, H. Dye-Sensitized Solar Cells. *Chem. Rev.* **2010**, *110*, 6595−6663.
(3) O'Regan, B.; Grätzel, M. A Low-Cost, High-Efficiency Solar Cell Based on Dye-Sensitized. *Nature* **1991**, *353*, 737−740.
(4) Grätzel, M. Recent Advances in Sensitized Mesoscopic Solar Cells. *Acc. Chem. Res.* **2009**, *42*, 1788−1798.
(5) Robertson, N. Optimizing Dyes for Dye-Sensitized Solar Cells. *Angew. Chem., Int. Ed.* **2006**, *45*, 2338−2345.
(6) Yella, A.; Lee, H.-W.; Tsao, H. N.; Yi, C.; Chandiran, A. K.; Nazeeruddin, M. K.; Diau, E. W.-G.; Yeh, C.-Y.; Zakeeruddin, S. M.;

Grätzel, M. Porphyrin-Sensitized Solar Cells with Cobalt (II/III)− Based Redox Electrolyte Exceed 12% Efficiency. *Science* **2011**, *334*, 629−634.
(7) Wu, Y.; Zhu, W. Organic Sensitizers from D-pi-A to D-A-pi-A: Effect of the Internal Electron-Withdrawing Units on Molecular Absorption, Energy Levels and Photovoltaic Performances. *Chem. Soc. Rev.* **2013**, *42*, 2039−2058.
(8) Mishra, A.; Fischer, M. K.; Bäuerle, P. Metal - Free Organic Dyes for Dye - Sensitized Solar Cells: From Structure: Property Relationships to Design Rules. *Angew. Chem., Int. Ed.* **2009**, *48*, 2474−2499.
(9) Zhou, H.; Chen, Q.; Li, G.; Luo, S.; Song, T.-b.; Duan, H.-S.; Hong, Z.; You, J.; Liu, Y.; Yang, Y. Interface Engineering of Highly Efficient Perovskite Solar Cells. *Science* **2014**, *345*, 542−546.
(10) Duarte, A.; Pu, K.-Y.; Liu, B.; Bazan, G. C. Recent Advances in Conjugated Polyelectrolytes for Emerging Optoelectronic Applications. *Chem. Mater.* **2011**, *23*, 501−515.
(11) Jiang, H.; Taranekar, P.; Reynolds, J. R.; Schanze, K. S. Conjugated Polyelectrolytes: Synthesis, Photophysics, and Applications. *Angew. Chem., Int. Ed.* **2009**, *48*, 4300−4316.
(12) Mwaura, J. K.; Zhao, X.; Jiang, H.; Schanze, K. S.; Reynolds, J. R. Spectral Broadening in Nanocrystalline TiO_2 Solar Cells Based on Poly (P-Phenylene Ethynylene) and Polythiophene Sensitizers. *Chem. Mater.* **2006**, *18*, 6109−6111.
(13) Taranekar, P.; Qiao, Q.; Jiang, H.; Ghiviriga, I.; Schanze, K. S.; Reynolds, J. R. Hyperbranched Conjugated Polyelectrolyte Bilayers for Solar-Cell Applications. *J. Am. Chem. Soc.* **2007**, *129*, 8958−8959.
(14) Jiang, H.; Zhao, X.; Shelton, A. H.; Lee, S. H.; Reynolds, J. R.; Schanze, K. S. Variable-Band-Gap Poly (Arylene Ethynylene) Conjugated Polyelectrolytes Adsorbed on Nanocrystalline TiO_2: Photocurrent Efficiency as a Function of the Band Gap. *ACS Appl. Mater. Interfaces* **2009**, *1*, 381−387.
(15) Duan, C.; Zhang, K.; Zhong, C.; Huang, F.; Cao, Y. Recent Advances in Water/Alcohol-Soluble π-Conjugated Materials: New Materials and Growing Applications in Solar Cells. *Chem. Soc. Rev.* **2013**, *42*, 9071−9104.
(16) Liu, X.; Zhu, R.; Zhang, Y.; Liu, B.; Ramakrishna, S. Anionic Benzothiadiazole Containing Polyfluorene and Oligofluorene as Organic Sensitizers for Dye-Sensitized Solar Cells. *Chem. Commun.* **2008**, 3789−3791.
(17) Kanimozhi, C.; Balraju, P.; Sharma, G.; Patil, S. Diketopyrrolopyrrole-Based Donor− Acceptor Copolymers as Organic Sensitizers for Dye Sensitized Solar Cells. *J. Phys. Chem. C* **2010**, *114*, 3287−3291.
(18) Fang, Z.; Eshbaugh, A. A.; Schanze, K. S. Low-Bandgap Donor-Acceptor Conjugated Polymer Sensitizers for Dye-Sensitized Solar Cells. *J. Am. Chem. Soc.* **2011**, *133*, 3063−3069.
(19) Warnan, J.; Pellegrin, Y.; Blart, E.; Odobel, F.; Zhang, W.; Liu, B.; Babu, V. J.; Ramakrishna, S. Application of poly-(3-hexylthiophene) Functionalized with an Anchoring Group in Dye - Sensitized Solar Cells. *Macromol. Rapid Commun.* **2011**, *32*, 1190−1194.
(20) An, B.-K.; Mulherin, R.; Langley, B.; Burn, P.; Meredith, P. Ruthenium Complex-Cored Dendrimers: Shedding Light on Efficiency Trade-Offs in Dye-Sensitised Solar Cells. *Org. Electron.* **2009**, *10*, 1356−1363.
(21) Thongkasee, P.; Thangthong, A.; Janthasing, N.; Sudyoadsuk, T.; Namuangruk, S.; Keawin, T.; Jungsuttiwong, S.; Promarak, V. Carbazole-Dendrimer-Based Donor-Pi-Acceptor Type Organic Dyes for Dye-Sensitized Solar Cells: Effect of the Size of the Carbazole Dendritic Donor. *ACS Appl. Mater. Interfaces* **2014**, *6*, 8212−8222.
(22) Feng, F.; Yang, J.; Xie, D.; McCarley, T. D.; Schanze, K. S. Remarkable Photophysics and Amplified Quenching of Conjugated Polyelectrolyte Oligomers. *J. Phys. Chem. Lett.* **2013**, *4*, 1410−1414.
(23) Koenen, J.-M.; Zhu, X.; Pan, Z.; Feng, F.; Yang, J.; Schanze, K. S. Enhanced Fluorescence Properties of Poly (Phenylene Ethynylene)-Conjugated Polyelectrolytes Designed to Avoid Aggregation. *ACS Macro Lett.* **2014**, *3*, 405−409.
(24) Zhao, X.; Jiang, H.; Schanze, K. S. Polymer Chain Length Dependence of Amplified Fluorescence Quenching in Conjugated Polyelectrolytes. *Macromolecules* **2008**, *41*, 3422−3428.
(25) Lee, S.-H. A.; Abrams, N. M.; Hoertz, P. G.; Barber, G. D.; Halaoui, L. I.; Mallouk, T. E. Coupling of Titania Inverse Opals to Nanocrystalline Titania Layers in Dye-Sensitized Solar Cells. *J. Phys. Chem. B* **2008**, *112*, 14415−14421.
(26) Jiang, H.; Zhao, X.; Shelton, A. H.; Lee, S. H.; Reynolds, J. R.; Schanze, K. S. Variable-Band-Gap Poly(Arylene Ethynylene) Conjugated Polyelectrolytes Adsorbed on Nanocrystalline TiO_2: Photocurrent Efficiency as a Function of the Band Gap. *ACS Appl. Mater. Interfaces* **2009**, *1*, 381−387.
(27) Odian, G. *Principles of Polymerization*; Wiley: New York, 2004.
(28) Liu, T.; Rulkens, R.; Wegner, G.; Chu, B. Laser Light Scattering Study of a Rigid-Rod Polyelectrolyte. *Macromolecules* **1998**, *31*, 6119−6128.
(29) Yang, R.; Garcia, A.; Korystov, D.; Mikhailovsky, A.; Bazan, G. C.; Nguyen, T.-Q. Control of Interchain Contacts, Solid-State Fluorescence Quantum Yield, and Charge Transport of Cationic Conjugated Polyelectrolytes by Choice of Anion. *J. Am. Chem. Soc.* **2006**, *128*, 16532−16539.
(30) Sedlak, M.; Amis, E. J. Dynamics of Moderately Concentrated Salt-Free Polyelectrolyte Solutions - Molecular-Weight Dependence. *J. Chem. Phys.* **1992**, *96*, 817−825.
(31) Li, Y.; Xia, J.; Dubin, P. L. Complex Formation between Polyelectrolyte and Oppositely Charged Mixed Micelles: Static and Dynamic Light Scattering Study of the Effect of Polyelectrolyte Molecular Weight and Concentration. *Macromolecules* **1994**, *27*, 7049−7055.
(32) Feng, L. H.; Zhu, C. L.; Yuan, H. X.; Liu, L. B.; Lv, F. T.; Wang, S. Conjugated Polymer Nanoparticles: Preparation, Properties, Functionalization and Biological Applications. *Chem. Soc. Rev.* **2013**, *42*, 6620−6633.
(33) Zhu, X.; Nepomnyashchii, A. B.; Roitberg, A. E.; Parkinson, B. A.; Schanze, K. S. Photosensitization of Single-Crystal ZnO by a Conjugated Polyelectrolyte Designed to Avoid Aggregation. *J. Phys. Chem. Lett.* **2013**, *4*, 3216−3220.
(34) Zhao, X.; Pinto, M. R.; Hardison, L. M.; Mwaura, J.; Muller, J.; Jiang, H.; Witker, D.; Kleiman, V. D.; Reynolds, J. R.; Schanze, K. S. Variable Band Gap Poly(Arylene Ethynylene) Conjugated Polyelectrolytes. *Macromolecules* **2006**, *39*, 6355−6366.
(35) Tan, C.; Pinto, M. R.; Schanze, K. S. Photophysics, Aggregation and Amplified Quenching of a Water-Soluble Poly (Phenylene Ethynylene). *Chem. Commun.* **2002**, 446−447.
(36) Wang, F.; Bazan, G. C. Aggregation-Mediated Optical Properties of Ph-Responsive Anionic Conjugated Polyelectrolytes. *J. Am. Chem. Soc.* **2006**, *128*, 15786−15792.
(37) Chen, K. S.; Liu, W. H.; Wang, Y. H.; Lai, C. H.; Chou, P. T.; Lee, G. H.; Chen, K.; Chen, H. Y.; Chi, Y.; Tung, F. C. New Family of Ruthenium - Dye - Sensitized Nanocrystalline TiO_2 Solar Cells with a High Solar - Energy - Conversion Efficiency. *Adv. Funct. Mater.* **2007**, *17*, 2964−2974.
(38) Wang, Z.-S.; Cui, Y.; Dan-Oh, Y.; Kasada, C.; Shinpo, A.; Hara, K. Thiophene-Functionalized Coumarin Dye for Efficient Dye-Sensitized Solar Cells: Electron Lifetime Improved by Coadsorption of Deoxycholic Acid. *J. Phys. Chem. C* **2007**, *111*, 7224−7230.
(39) Lu, H.-P.; Tsai, C.-Y.; Yen, W.-N.; Hsieh, C.-P.; Lee, C.-W.; Yeh, C.-Y.; Diau, E. W.-G. Control of Dye Aggregation and Electron Injection for Highly Efficient Porphyrin Sensitizers Adsorbed on Semiconductor Films with Varying Ratios of Coadsorbate. *J. Phys. Chem. C* **2009**, *113*, 20990−20997.
(40) Wang, Z.-S.; Koumura, N.; Cui, Y.; Takahashi, M.; Sekiguchi, H.; Mori, A.; Kubo, T.; Furube, A.; Hara, K. Hexylthiophene-Functionalized Carbazole Dyes for Efficient Molecular Photovoltaics: Tuning of Solar-Cell Performance by Structural Modification. *Chem. Mater.* **2008**, *20*, 3993−4003.
(41) Marinado, T.; Nonomura, K.; Nissfolk, J.; Karlsson, M. K.; Hagberg, D. P.; Sun, L.; Mori, S.; Hagfeldt, A. How the Nature of Triphenylamine-Polyene Dyes in Dye-Sensitized Solar Cells Affects the Open-Circuit Voltage and Electron Lifetimes. *Langmuir* **2010**, *26*, 2592−2598.

DOI: 10.1021/acsami.5b04162
ACS Appl. Mater. Interfaces 2015, 7, 16601−16608